Bone 127 (2019) 228–243

Contents lists available at ScienceDirect

Bone

journal homepage: www.elsevier.com/locate/bone

Full Length Article

New explanation for autosomal dominant high bone mass: Mutation of low-density lipoprotein receptor-related protein 6☆,☆☆

Michael P. Whyte[a,b,*], William H. McAlister[c], Fan Zhang[a], Vinieth N. Bijanki[a], Angela Nenninger[a], Gary S. Gottesman[a], Elizabeth L. Lin[a,b], Margaret Huskey[b], Shenghui Duan[b], Kathryn Dahir[d], Steven Mumm[a,b]

[a] Center for Metabolic Bone Disease and Molecular Research, Shriners Hospitals for Children – St. Louis, St. Louis, MO 63110, USA
[b] Division of Bone and Mineral Diseases, Department of Internal Medicine, Washington University School of Medicine at Barnes-Jewish Hospital, St. Louis, MO 63110, USA
[c] Mallinckrodt Institute of Radiology, Washington University School of Medicine at St. Louis Children's Hospital, St. Louis, MO 63110, USA
[d] Department of Endocrinology and Diabetes, Vanderbilt University Medical Center, Nashville, TN 37232, USA

ARTICLE INFO

Keywords:
Albers-Schönberg disease
Bone modeling
β-Catenin
Chiari I malformation
Creatine kinase
DXA
Endosteum
Exostosis
High resolution computed tomography
Hyperostosis
Lactate dehydrogenase
LRP5
LRP6
Osteopetrosis
Osteosclerosis
Sclerostin
Skeletal dysplasia
Torus palatinus
Translational research
Wnt signaling

ABSTRACT

LRP5 encodes low-density lipoprotein receptor-related protein 5 (LRP5). When LRP5 with a Frizzled receptor join on the surface of an osteoblast and bind a member of the Wnt family of ligands, canonical Wnt/β-catenin signaling occurs and increases bone formation. Eleven heterozygous gain-of-function missense mutations within *LRP5* are known to prevent the LRP5 inhibitory ligands sclerostin and dickkopf1 from attaching to LRP5's first β-propeller, and thereby explain the rare autosomal dominant (AD) skeletal disorder "high bone mass" (HBM). LRP6 is a cognate co-receptor of LRP5 and similarly controls Wnt signaling in osteoblasts, yet the consequences of increased LRP6-mediated signaling remain unknown.

We investigated two multi-generational American families manifesting the clinical and routine laboratory features of *LRP5* HBM but without an *LRP5* defect and instead carrying a heterozygous *LRP6* missense mutation that would alter the first β-propeller of LRP6. In Family 1 *LRP6* c.602C > T, p.A201V was homologous to *LRP5* HBM mutation c.641C > T, p.A214V, and in Family 2 *LRP6* c.553A > C, p.N185H was homologous to *LRP5* HBM mutation c.593A > G, p.N198S but predicting a different residue at the identical amino acid position. In both families the *LRP6* mutation co-segregated with striking generalized osteosclerosis and hyperostosis. Clinical features shared by the seven *LRP6* HBM family members and ten *LRP5* HBM patients included a broad jaw, torus palatinus, teeth encased in bone and, reportedly, resistance to fracturing and inability to float in water. For both HBM disorders, all affected individuals were taller than average for Americans (Ps < 0.005), but with similar mean height Z-scores (P = 0.7606) and indistinguishable radiographic skeletal features. Absence of adult maxillary lateral incisors was reported by some *LRP6* HBM individuals. In contrast, our 16 patients with AD osteopetrosis [i.e., Albers-Schönberg disease (A-SD)] had an unremarkable mean height Z-score (P = 0.9401) lower than for either HBM group (Ps < 0.05). DXA mean BMD Z-scores in *LRP6* HBM versus *LRP5* HBM were somewhat higher at the lumbar spine (+7.8 vs +6.5, respectively; P = 0.0403), but no different at the total hip (+7.9 vs +7.7, respectively; P = 0.7905). Among the three diagnostic groups, only the *LRP6* HBM DXA BMD values at the spine seemed to increase with subject age (R = +0.7183, P = 0.0448). Total hip BMD Z-scores were not significantly different among the three disorders (Ps > 0.05), and showed no age effect (Ps > 0.1). HR-pQCT available only for *LRP6* HBM revealed indistinct corticomedullary boundaries, high distal forearm and tibial total volumetric BMD, and finite element analysis predicted marked fracture resistance.

Hence, we have discovered mutations of *LRP6* that cause a dento-osseous disorder indistinguishable without

☆ Funded in part by: Shriners Hospitals for Children, The Clark and Mildred Cox Inherited Metabolic Bone Disease Research Fund and The Hypophosphatasia Research Fund at The Barnes-Jewish Hospital Foundation, and the National Institute of Diabetes and Digestive and Kidney Diseases of the National Institutes of Health (NIH) under Award Number DK067145. The content of the manuscript is solely the responsibility of the authors and does not necessarily represent the official views of the NIH.

☆☆ Presented in part at: American Society for Bone and Mineral Research 2018 Annual Meeting, September 28–October 1, 2018, Montreal, Canada [J Bone Miner Res 33 (Suppl 1): 57, 2018].

* Corresponding author at: Shriners Hospitals for Children – St. Louis, 4400 Clayton Avenue, St. Louis, MO 63110, USA.
E-mail addresses: mwhyte@shrinenet.org (M.P. Whyte), mcalisterw@wustl.edu (W.H. McAlister), fzhang@shrinenet.org (F. Zhang), vbijanki@shrinenet.org (V.N. Bijanki), anenninger@shrinenet.org (A. Nenninger), ggottesman@shrinenet.org (G.S. Gottesman), elin24@wustl.edu (E.L. Lin), huskeym@wustl.edu (M. Huskey), sduan@wustl.edu (S. Duan), kathryn.dahir@Vanderbilt.Edu (K. Dahir), smumm@wustl.edu (S. Mumm).

https://doi.org/10.1016/j.bone.2019.05.003
Received 26 March 2019; Received in revised form 1 May 2019; Accepted 3 May 2019
Available online 11 May 2019

mutation analysis from *LRP5* HBM. *LRP6* HBM seems associated with generally good health, providing some reassurance for the development of anabolic treatments aimed to enhance LRP5/LRP6-mediated osteogenesis.

1. Introduction

Heritable forms of osteosclerosis and hyperostosis [1] (trabecular and cortical bone excess, respectively) [2] include the osteopetroses (OPTs) caused by loss-of-function mutations of genes essential for osteoclast (OC)-mediated skeletal resorption and "high bone mass" (HBM) due to heterozygous gain-of-function missense mutations within *LRP5* that encodes low-density lipoprotein receptor-related protein 5 (LRP5) important for osteoblast (OB)-mediated bone formation [3,4]. When LRP5 with a Frizzled receptor on the OB surface bind a member of the Wnt family, canonical Wnt/β-catenin signaling enhances osteogenesis [5,6]. Conversely, Wnt/β-catenin signaling and bone formation are diminished if either of the inhibitory ligands sclerostin (SOST) or dickkopf1 (DKK1) couples to the first β-propeller of LRP5 [7–9]. To date, 11 heterozygous missense mutations within *LRP5* impair SOST/DKK1 binding to LRP5 and thereby cause HBM [10–17]. For some time, HBM has incorrectly been considered an autosomal dominant (AD) form of OPT [18] (OMIM #144750) [1]. Among the OPTs, including its one true AD form, Albers-Schönberg disease (A-SD) due to heterozygous loss-of-function mutation of the gene *CLCN7* encoding chloride channel 7 [19] (OMIM #166600) [1], bone modeling (shaping) and strength are compromised by the OC failure [3]. Conversely, in *LRP5* HBM (OMIM #607634) [1] OB stimulation leads to properly-shaped and fracture-resistant bones [10–17]. Therefore, Wnt/β-catenin signaling harbors potential targets for treatment of skeletal disease, including osteoporosis [9,20]. However, the *LRP5* HBM phenotype suggests caution as it ranges from non-syndromic [10,21], to syndromic with a broad jaw and torus palatinus [11], to overt disease with oropharyngeal exostoses that encase teeth, Chiari I malformation, and cranial nerve palsies [13,15,22].

LRP6 and LRP5 are cognate co-receptors [23]. On the OB surface, LRP6 acts similarly but independently of LRP5 [5,6] yet gain-of-function mutations of *LRP6* and any clinical consequences remain undiscovered.

Here, in two multigenerational American families, we delineate the first two mutations of *LRP6* associated with a dento-osseous disorder that otherwise seems indistinguishable from *LRP5* HBM.

2. Materials and methods

2.1. Families

The two families with *LRP6* HBM are Caucasian. Their medical histories, detailed in the Supplementary Appendix, recount investigations after the dense mandible of a teenage girl was discovered in Family 1 and the dense skull of a boy was discovered in Family 2 (Fig. 1).

Informed written consent, approved both by the Human Research Protection Office, Washington University School of Medicine, St. Louis, MO, and Medical Research Department, Shriners Hospitals for Children, Tampa, FL, USA, preceded all investigational studies. The two families totaled seven affected and four unaffected individuals evaluated at the Center for Metabolic Bone Disease and Molecular Research, Shriners Hospitals for Children – St. Louis; St. Louis, MO, USA (Research Center). Family 1 from Kentucky was studied in 2015 and 2018, and Family 2 from Missouri was studied in 2018. Over a longer timeframe, we had similarly investigated 10 children or adults from nine families with *LRP5* HBM and 16 children or adults from 13 families with A-SD. The age ranges of the *LRP6* HBM, *LRP5* HBM, and A-SD patients were 5–57 years, 9–74 years, and 4–43 years, respectively.

2.1.1. Family 1

The proposita (III-1: Fig. 1A), 19 years-of-age, was found in 2014 by her orthodontist to have a radiographically dense mandible. Her adult maxillary lateral incisors were congenitally missing, and she believed her wisdom teeth never formed. She was healthy and reported no bone

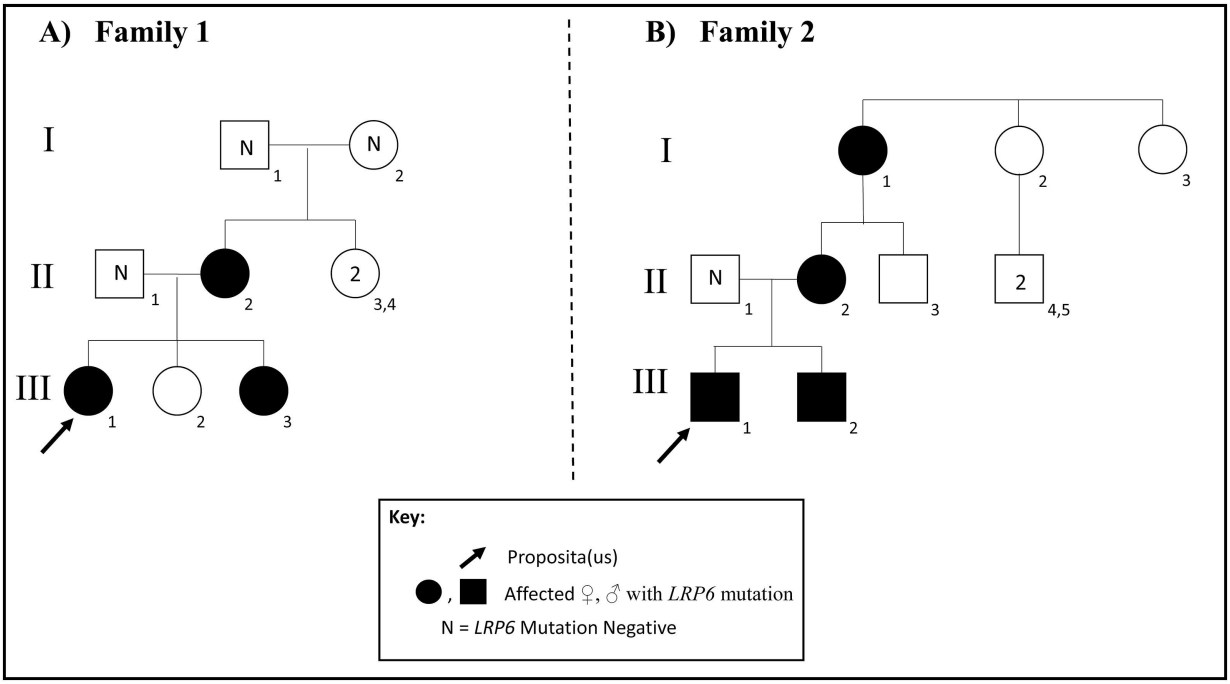

Fig. 1. Pedigrees of *LRP6* high bone mass families 1 and 2.

pain, fractures, or symptoms of cranial nerve compression. A broad jaw and torus palatinus were apparent (Fig. 2A).

Her sister (III-3: Fig. 1A), 15 years-of-age, reported polycystic ovary syndrome and fused mandibular central incisors but no absence of maxillary lateral incisors. Sharp knee pain could follow sporting activities. She had never fractured. Orthodontia had been uncomplicated.

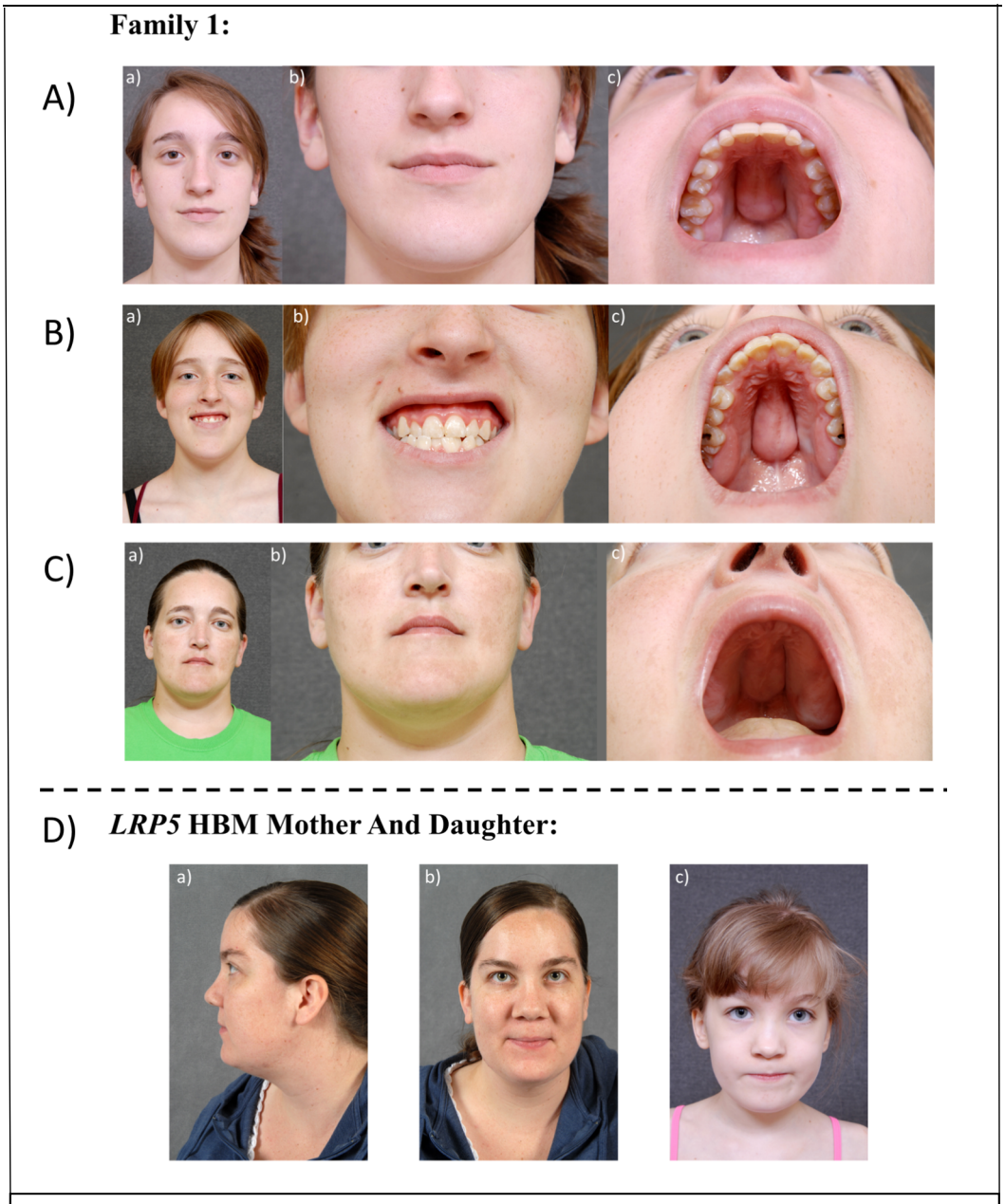

A) Proposita (III-1, Figure 1A): She has a,b) a broad jaw and c) torus palatinus with lingual exostoses and no maxillary lateral incisors.
B) Sister (III-3, Figure 1A): She has a,b) a broad jaw and c) torus palatinus, and exostoses, but no absence of her maxillary lateral incisors.
C) Sisters' mother (II-1, Figure 1A): She has a,b) a broad jaw, but c) no torus palatinus following its removal to fit dentures.
D) In *LRP5* HBM Family 9 (Table 1), a,b) this 25-year-old woman and c) her 9-year-old daughter have a broad jaw resembling the *LRP6* HBM families **(see also Figure 3)**.

Fig. 2.

She had a wide jaw and torus palatinus (Fig. 2B).

The proposita's and sister's mother (II-2: Fig. 1A), 43 years-of-age, reported congenital absence of her adult maxillary lateral incisors. She had never fractured and said she could not float in water. Patella dislocation had been surgically repaired. Nuchal pain could occur if she extended her neck. There were no cranial nerves symptoms. Estradiol had been taken for two years for menorrhagia. Her torus palatinus had been "chiseled off" four years earlier to fit complete dentures. Bone had also twice been "shaved off" near anterior teeth. Her jaw was broad (Fig. 2C).

The broad jaw of these three individuals resembled the same finding in *LRP5* HBM (Fig. 2D).

2.1.2. Family 2

Reportedly, at least five generations of this family (propositus, mother, maternal grandmother, great-grandmother, and great-great-grandmother) had torus palatinus with congenitally absent adult maxillary lateral incisors (Fig. 1B).

The propositus (III-1: Fig. 1B), 8 years-of-age, was healthy but had recently suffered transient traumatic right facial nerve palsy lasting two months. Computed tomography (CT) of his head and subsequently a radiographic skeletal survey were reported to show OPT. He denied skeletal symptoms, past fractures, or significant dental problems. However, headaches occurred twice or thrice weekly. Torus palatinus was present, but not prominent, and perhaps because of his young age his jaw was not broad (Fig. 3A, B). A recent panorex study had shown absence of his adult maxillary lateral incisors (Supplementary Appendix).

His healthy younger brother (III-2: Fig. 1B), 5 years-of-age, carried the family's *LRP6* mutation, but had neither a torus palatinus nor broad jaw. He had fallen down a flight of stairs at age 3 years, but did not break bones.

The mother (II-2: Fig. 1B), 35 years-of-age, reported epilepsy following head trauma as a child. She had bone pain, migraine headaches including teichopsia, 18° scoliosis, a large exostosis at a knee, torus palatinus, missing adult maxillary lateral incisors (Fig. 3C), and said she could not float. Her brother (II-3: Fig. 1B) reportedly had no torus and had broken several bones.

The propositus' maternal grandmother (I-1: Fig. 1B), 57 years-of-age, had torus palatinus and tori near her anterior teeth, migraine

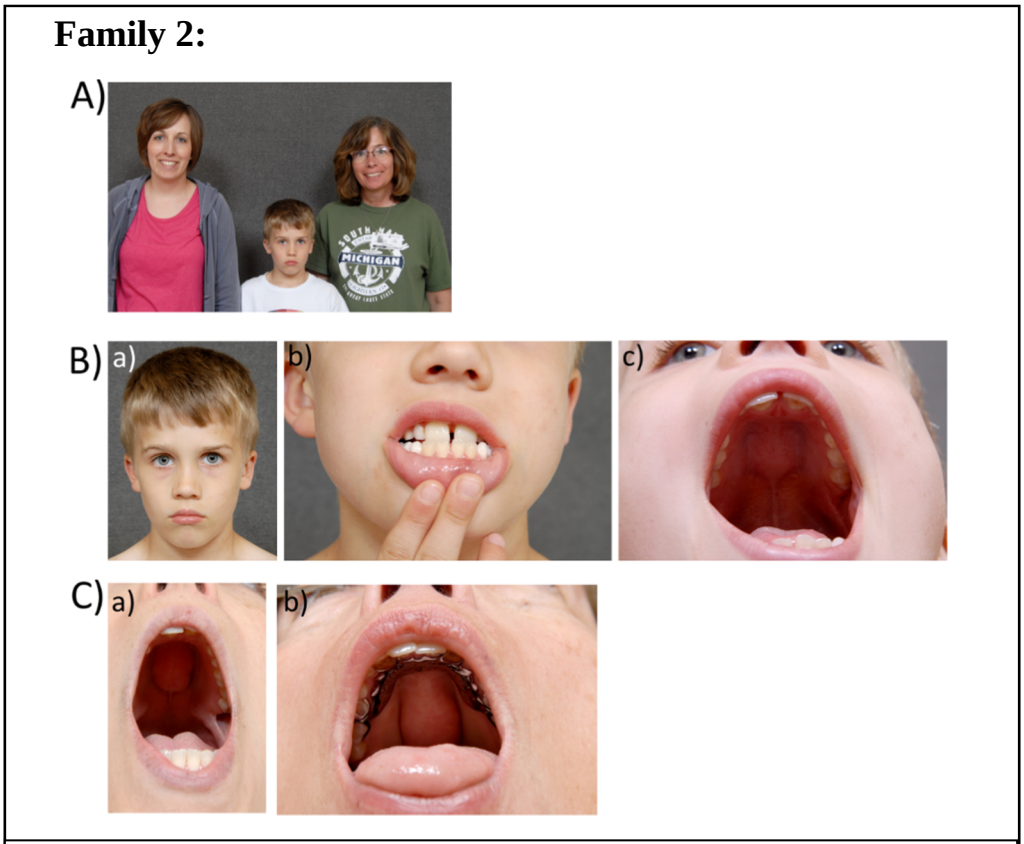

A) The propositus (center), affected mother (left), and affected maternal grandmother (right).
B) The propositus **(III-1: Figure 1B)** has a) a normally shaped jaw, b) absence of adult maxillary lateral incisors, and c) torus palatinus.
C) a) The propositus' mother **(II-2: Figure 1B)** has a) a torus palatinus. The maternal grandmother **(I-1: Figure 1B)** had b) undergone torus palatinus reduction to fit dentures, and also removal of exostoses near her anterior teeth.

Fig. 3.

Table 1
LRP6 and *LRP5* high bone mass and Albers-Schönberg disease study subjects.

Gene	Family	Study Subject	Gender+	Age (yr)	Height (cm)	Weight (kg)	BMD Z-score Spine	BMD Z-score Hip	Mutation
LRP6	1	A III-1**	F	17	170	70	+ 5.7	+ 7.6	Exon 3: c.602C>T, p.A201V
	″	B III-3**	F	13	164	46	+ 5.2	+ 8.6	″ ″ ″
	″	C II-2**	F	40	171	112	+ 9.4	+ 10.1	″ ″ ″
	″	″ ″	F	43	169	112	+ 10.0	+ 11.1	″ ″ ″
	2	A III-1‡	M	8	135	31	+ 8.8	+ 8.8	Exon 3: c.553A>C, p.N185H
	″	B III-2‡	M	5	116	22	+ 7.3	+ 7.5	″ ″ ″
	″	C II-2‡	F	35	169	70	+ 8.1	+ 6.4	″ ″ ″
	″	D I-1‡	F	57	166	77	+ 10.3	+ 6.4	″ ″ ″
LRP5	3	A	F	37	165	62	+ 7.4	+ 6.1 *	Exon 3: c.512G>T, p.Gly171Val
	4	A	F	58	175	113	+ 8.7	+ 8.5	Exon 2: c.461G>T, p.Arg154Met
	5	A	F	49	180	118	+ 6.1	+ 7.8	Exon 3: c.640G>A, p.Ala214Thr
	6	A	F	50	169	57	+ 5.4	+ 6.7 *	Exon 3: c.512G>T, p.Gly171Val
	″	″	F	53	169	59	+ 5.5 *	+ 6.0 *	″ ″ ″
	7	A	M	43	183	104	+ 8.6	+ 11.7	Exon 3: c.640G>A, p.Ala214Thr
	8	A	F	51	175	99	+ 6.5	+ 5.7	Exon 3: c.512G>T, p.Gly171Val
	9	A	F	9	134	28	+ 5.0	+ 5.3	Exon 3: c.640G>A, p.Ala214Thr
	″	B	F	13	165	67	+ 7.2	--	″ ″ ″
	″	″	F	25	167	108	+ 8.8	+ 9.3	″ ″ ″
	10	A	M	43	--	--	+ 4.1	+ 10.3	Exon 4: c.724G>A, p.Ala242Thr
	″	B	M	74	--	--	--	+ 5.4	″ ″ ″
	11	A	F	25	173	96	+ 6.4	+ 6.8	Exon 3: c.593A>G, p.Asn198Ser
A-SD	12	A	M	43	180	88	+ 5.2 *	+ 9.1 *	Exon 7: c.641A>G, p.Asn214Ser
	13	A	F	41	173	120	--	+ 10.1	Exon 25: c.2385_2386delAG, p.Gly796fs
	14	A	M	17	185	69	+ 8.6	+ 6.4	Exon 10: c.857G>A, p.Arg286Gln
	15	A	M	9	146	39	+ 9.9	+ 9.7	Exon 7: c.643G>A, p.Gly215Arg
	″	B	F	33	166	64	+ 9.5	+ 6.7	″ ″ ″
	″	C	M	36	173	69	+ 14.9	+ 10.0	″ ″ ″
	16	A	F	36	155	63	+ 14.8	--	Exon 24: c.2300G>T, p.Arg767Leu
	17	A	F	17	152	43	+ 8.8	+ 8.1	Exon 9: c.746C>A, p.Pro249Gln
	18	A	M	31	181	75	+ 11.6	+ 10.1	Exon 25: c.2332-1G>A, splice site
	19	A	M	20	182	85	+ 12.0	+ 7.8	Exon 9: c.746C>A, p.Pro249Gln
	20	A	M	4	101	15	- 1.4	--	Exon 13: c.1147_1148insA, p.Val383fs
	″	B	M	39	175	86	+ 12.1	+ 10.3	″ ″ ″
	21	A	M	8	131	27	+ 9.6	+ 6.5	Exon 8: c.689A>G, p.Lys230Arg
	22	A	M	16	176	73	+ 6.8	+ 7.8	Exon 22: splice site
	23	A	F	18	162	58	+ 7.1	+ 9.1	Exon 10: c.856C>T, p.Arg286Trp
	24	A	M	20	168	57	+ 9.1	+ 9.8	Exon 23: splice site

+ F = female, M = male

*GE Medical Systems Lunar Instrument

** Figure 1A

‡ Figure 1B

headaches about five times yearly, but no deafness, vision loss, or facial palsy. She described no bone pain, had never fractured despite tumbles playing sports as a teenager, and said empathically she could not float although her father could. Reportedly, her two sisters (I-2, 3: Fig. 1B) had no torus palatinus and could float.

The propositus' deceased maternal great grandmother (1931–2005) (Not Shown: Fig. 1B) had her torus palatinus "chiseled off" in middle-age to fit dentures, and was said to lack adult maxillary lateral incisors. Unilateral deafness had been attributed to some problem during childhood.

The propositus' deceased maternal great, great grandmother (1911–1993) (Not Shown: Fig. 1B) had, as a young woman, slipped on ice and fell beneath a parked car and "should have broken a leg". Reportedly, radiographs showed "marble bones" that were still present at her only follow-up one year later. The family had become familiar with the eponym "Albers-Schönberg disease". She too was said to lack adult maxillary lateral incisors. The medical histories of her five siblings were not known, except that her youngest brother had broken an arm in high school.

2.2. Biochemical studies

Biochemical testing of all study subjects used blood collected after an overnight fast and 24-hour urine specimens. Our methodologies during this timeframe are published for the routine studies of mineral and skeletal homeostasis, as well as for the biochemical markers of bone turnover [24,25]. A "lipid panel" (LabCorp, Dublin, OH, USA) evaluated both affected sisters in Family 1 and the affected mother and grandmother in Family 2 for any lipid abnormalities due to *LRP6* mutation (see Discussion).

2.3. Radiological studies

To identify and then contrast the radiographic skeletal findings of *LRP6* HBM to *LRP5* HBM (but not to A-SD), the available images (sometimes skeletal surveys) from those with *LRP6* HBM and those with *LRP5* HBM were first randomly assessed blinded to the molecular diagnosis. Then, unblinded images from the senior individuals in both groups (ages 43–74 years) were contrasted for any feature(s) that distinguished between the two disorders.

Dual-energy X-ray absorptiometry (DXA) had been performed routinely at the Research Center sequentially using QDR1000, QDR4500A, Discovery A, and Horizon instruments that had not been cross-calibrated (Hologic Inc., Waltham, MA, USA). For three consultand individuals with *LRP5* HBM and one with A-SD, DXA was obtained with a Lunar instrument (GE Medical Systems, Inc., Waukesha, WI, USA) (Table 1). BMD Z-scores for the lumbar spine ("spine") and non-dominant total hip ("hip") were those generated routinely by the DXA instrument's software. When multiple DXA assessments had been obtained for a given individual, we analyzed only the single most complete study for comparisons among the three diagnostic groups, but used all subject values for age-effect regression analyses for the individual disorders (see Statistical Analyses).

In 2018, high-resolution peripheral quantitative computed tomography (HR-pQCT) using the second generation XtremeCTII instrument (Scanco Medical, Bruttisellen, Switzerland) became available to us. Both distal radii and tibias of the affected members of Families 1 and 2 were studied. We used the midpoint of the ultra distal end of the epiphysis as the anatomical reference line. Then, 10.24 mm sections (with 168 slices) were scanned starting at 9.0 mm proximal to the radius reference line, and 22.5 mm proximal to the tibia reference line [26]. All scans were graded [1–5] for motion [27], and those grade 2 and better were analyzed. Cortical and trabecular parameters were explored using the instrument's segmentation method and standard morphological analysis. Micro Finite Element Analysis (μFEA) was performed using the instrument's μFEA solver [28].

2.4. Mutation analyses

Peripheral blood leukocyte DNA was obtained from all study subjects using the Puregene DNA Extraction Kit (Gentra Systems, Minneapolis, MN, USA). The diagnosis of *LRP6* HBM or *LRP5* HBM or A-SD was established by mutation analysis in our research laboratory. *LRP5* mutation detection was performed as previously published [13,15]. *LRP6* exons 2–4 were PCR amplified and Sanger-sequenced using primers we designed and available upon request.

In Family 1, we first Sanger-sequenced *LRP5* exons 2–4 for the proposita anticipating a diagnosis of *LRP5* HBM. When this proved negative, we performed Ion Torrent (Thermo Fisher Scientific, Waltham, MA, USA) next generation sequencing (NGS) for 35 genes that: i) cause osteosclerotic disorders, ii) condition skeletal remodeling, or iii) reflect mouse models with skeletal features of HBM: i.e., *LRP4*, *LRP5*, *LRP6*, *CLCN7*, *TNFRSF11A* (*RANK*), *TNFRSF11B* (*OPG*), *TNFSF11* (*RANKL*), *VCP*, *SQSTM1*, *TGFB1*, *IFITM5*, *MAFB*, *CSF1*, *CSFR1*, *TRAF6*, *RELA*, *RELB*, *REL*, *NFKB1*, *NFKB2*, *TFEB*, *CA2*, *CTSK* (*CATHEPSIN K*), *OSTM1*, *PLEKHM1*, *TCIRG1*, *SOST*, *SLC29A3*, *SNX10*, *FAM20C*, *FAM123B* (*AMER1*), *TYROBP*, *LEMD3*, *DLX3*, and *PTDSS1* [3,4]. The proposita's *LRP6* variant revealed by Ion Torrent was then verified by Sanger sequencing.

In Family 2, we first Sanger-sequenced *LRP5* exons 2–4 in the affected mother. When this proved negative, we Sanger-sequenced her homologous *LRP6* exons 2–4.

Subsequently, *LRP6* exon 3, where both *LRP6* mutations were identified, was Sanger-sequenced for other members of the two families.

2.5. Statistical analyses

Height Z-scores were calculated using the SAS program downloaded from the US Centers for Disease Control and Prevention (CDC) growth chart website (https://www.cdc.gov/nccdphp/dnpao/growthcharts/resources/sas.htm) reflecting sex-matched Americans ages 0–20 years. For our study subjects older than age 20 years, we applied the reference values for age 20 years. All statistical analyses and graphics were performed using SAS software 9.3 (SAS Institute Inc., Cary, NC, USA). The one-sample *t*-test, with null hypothesis mean = 0 for the normal population, was used to compare patient mean height and mean BMD Z-scores. Regression analysis determined if the total of the spine or hip BMD Z-scores separately showed any age-effect. The general linear model (GLM) contrasted the mean height and mean BMD Z-scores for the *LRP6* HBM, *LRP5* HBM, and A-SD groups after adjusting for any age effects. A two-sided P-value < 0.05 was considered statistically significant.

3. Results

Data were available from seven affected individuals in the two families with *LRP6* HBM, ten affected individuals in the nine families with *LRP5* HBM, and 16 affected individuals in the 13 families with A-SD (Table 1).

3.1. Mutation analysis

In Family 1, Sanger sequencing of the proposita's *LRP5* exons 2–4, where *LRP5* HBM mutations are reported [10–15], was negative. Subsequently, our Ion Torrent NGS sequencing was negative for the 34 known elevated bone mass genes, but instead uniquely revealed a heterozygous *LRP6* missense variant (c.602C > T, p.A201V) in exon 3. The proposita's defect was confirmed by Sanger sequencing, and then identified in her sister and mother with HBM. Her father tested negative for both an *LRP5* and the *LRP6* mutation. The missense nucleotide change in their *LRP6* would alter its protein's first β-propeller where homologous *LRP5* HBM mutations had been documented. In fact,

Family 1's *LRP6* variant was precisely homologous to the *LRP5* HBM mutation (c.641C > T, p.A214V) [10] i.e., the same propeller and nucleotide and amino acid change (Fig. 4). The affected mother apparently represented de novo occurrence of *LRP6* HBM because her parents, who were not studied radiographically, etc., both tested negative for the *LRP6* mutation.

In Family 2, Sanger-sequencing of *LRP5* exons 2–4 of the affected mother was negative. Accordingly, we Sanger-sequenced exons 2–4 of *LRP6* and identified a heterozygous missense variant (c.553A > C, p.N185H) (Fig. 4). This *LRP6* mutation was homologous to the amino acid residue of a known *LRP5* HBM mutation [11], but encoded a unique amino acid variant (c.593A > G, p.N198S). Subsequently, the propositus' affected younger brother and affected maternal grandmother were shown to carry this *LRP6* defect. The propositus' father, without HBM, was *LRP6* and *LRP5* mutation negative.

To support our diagnosis of *LRP6* HBM, leukocyte DNA from the *LRP6* mutation-positive proposita of Family 1 (III-1: Fig. 1A) was evaluated for *LRP5* using Sanger sequencing in a commercial laboratory (Connective Tissue Gene Tests, Allentown, PA, USA). There, all coding exons of *LRP5* (NM_002335.2) were intact using MiSeq NGS (Illumina, San Diego, CA, USA).

3.2. Heights

Adult height data were available only for three women with *LRP6* HBM (mean ± SD = 169 ± 2.5 cm; 5 ft., 7in ± 1.0 in.) and seven women with *LRP5* HBM (mean ± SD = 172 ± 5.3 cm; 5 ft., 8 in ± 5.3 in.). All had above-average heights (Ps < 0.005), with the height of one person in both HBM groups being above the reference range (Fig. 5). In Family 1, the sisters' father's height was 182.4 cm (5 ft. 11.8 in) (Z-score +0.78) with DXA Z-scores of −0.3 hip and −0.5 for lumbar spine. In Family 2, the propositus' father's height was 181.1 cm (5 ft., 11.3 in.) (Z-score +0.6). Using the GLM, no difference was found between the mean height Z-scores of the two HBM groups (P = 0.7606). People with *LRP6* HBM or *LRP5* HBM were always taller than average for the American population (Ps < 0.005) and those with A-SD (Ps < 0.05) whose mean height Z-score of +0.02 was essentially average for Americans (P = 0.9401) (Table 2). In contrast to *LRP6* HBM and *LRP5* HBM, none of the 16 individuals with A-SD was taller than the reference range, and one had distinctly short stature (Z-score −3.0) (Fig. 5).

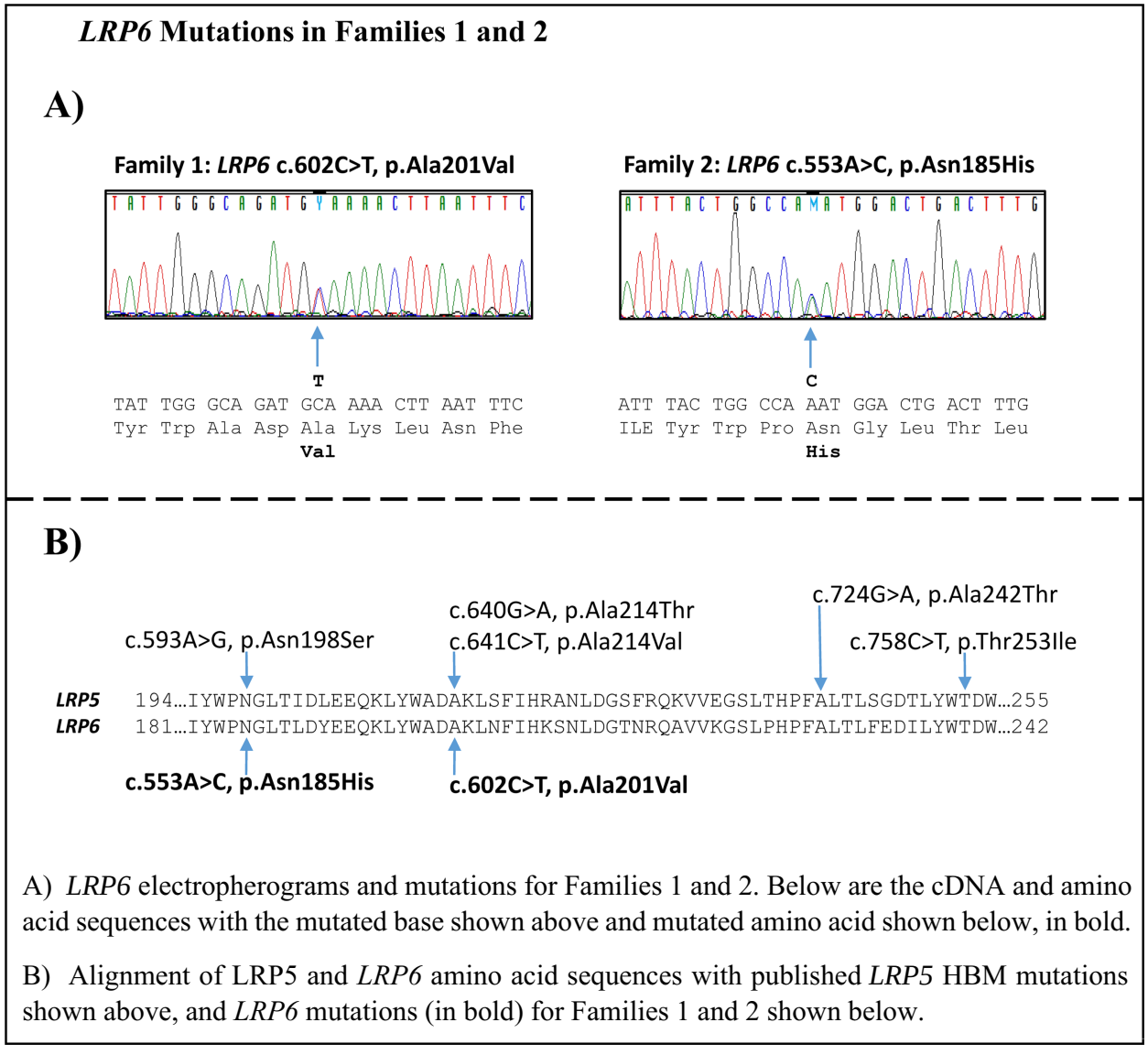

Fig. 4. *LRP6* mutations in Families 1 and 2.

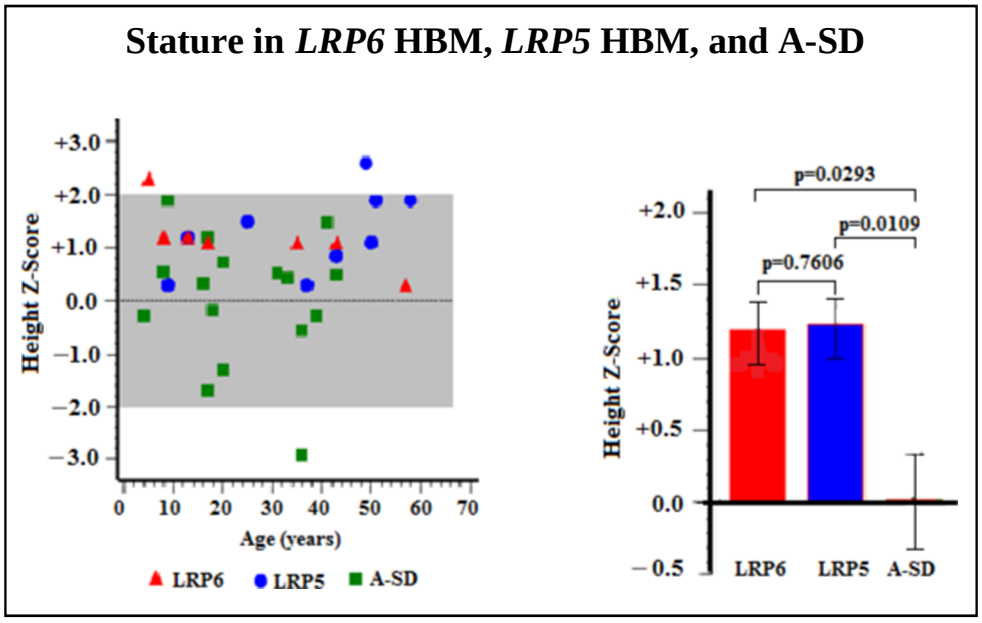

Fig. 5. Stature in *LRP6* HBM, *LRP5* HBM, and A-SD.

Table 2
Comparison of *LRP6* HBM, *LRP5* HBM, and A-SD height Z-scores to healthy Americans and among the three disorders.

Group	Mean (SD)	(min, max)	95%CI	P-value	
				$H_0 = 0$	Subgroup comparison
LRP6 (n = 7)	+1.2 (0.6)	+0.3, +2.3	+0.6, +1.7	0.0017	P = 0.7606 (LRP6 vs LRP5)
LRP5 (n = 9)	+1.3 (0.8)	+0.3, +2.6	+0.7, +1.9	0.0010	P = 0.0293 (LRP6 vs A-SD)
A-SD (n = 16)	+0.02 (1.2)	−3.0, +1.9	−0.6, +0.7	0.9401	P = 0.0109 (LRP5 vs A-SD)

3.3. Biochemical findings

In both Family 1 and 2 with *LRP6* HBM, routine studies of mineral homeostasis (including fasting serum levels of calcium, ionized calcium, phosphorus, magnesium, and intact parathyroid hormone (PTH) and 24-hour urine calcium/creatinine ratios) were normal for the three affected children and the three affected adults who were tested.

In 1996, we had reported that individuals with A-SD caused by defective CLCN7, but not individuals with *LRP5* HBM, typically have elevated serum levels of the brain isoenzyme of creatine kinase (BB-CK), perhaps released by their numerous and dysfunctional OCs in A-SD [29]. Then, in 2010, we reported that A-SD also features elevated serum aspartate transaminase (AST), tartrate-resistant acid phosphatase (TRAP), and lactate dehydrogenase (LDH) (isoenzymes 2, 3, 4), perhaps from disruption of plasma membrane integrity in multiple organs and tissues [30]. Herein, as for *LRP5* HBM, our *LRP6* HBM study subjects had normal circulating activity for each of these enzymes.

Despite the increased skeletal mass of the *LRP6* HBM subjects, their levels of the bone turnover markers osteocalcin, TRAP, bone-specific ALP, and procollagen type 1 N-terminal propeptide in serum as well as deoxypyridinoline in urine were typically normal for age. Serum C-terminal telopeptide of type 1 collagen was elevated in the three affected children tested, but normal in the three affected adults.

The lipid panel results were normal for the proposita in Family 1, but her affected younger sister with normal levels of serum cholesterol HDL and VLDL had elevated levels of total cholesterol, triglycerides, and LDL cholesterol. In Family 2, the propositus' affected mother's lipid panel was normal, but the affected grandmother had elevated total cholesterol and LDL cholesterol despite ongoing medical treatment for hyperlipidemia (Supplementary Appendix).

3.4. Radiological findings

The radiographic findings of *LRP5* HBM are reviewed in OMIM (#144750) [1].

3.4.1. Radiographic findings

We did not find any single or combinatory feature(s) that seemed to distinguish *LRP6* HBM from *LRP5* HBM. The principal shared radiographic changes, but showing a considerable range of severity, included: i) sclerosis of the entire skeleton, ii) uniformly thickened diploic space in the skull (sometimes appearing so dense it lacked a trabecular pattern), iii) poor development (aeration) of the frontal and maxillary sinuses, iv) radiodense orbital roofs, facial bones, and mandible having an obtuse angle and rounded body, v) teeth obscured by exostoses, vi) protrusion of the submental process, and vii) mild shaping defects of long bones with especially endosteal hyperostosis (Figs. 6 & 7). The vertebral bodies were diffusely sclerotic without striking accentuation of their superior and inferior end plates (i.e., no “rugger-jersey spine” appearance), thus differing *LRP6* HBM and *LRP5* HBM from A-SD [2–4]. *LRP6* HBM or *LRP5* HBM joint spaces could appear well preserved despite substantial nearby osteosclerosis that in A-SD perhaps explains associated osteoarthritis [31]. The excess bone that often obscured especially posterior teeth seemed more prevalent but less severe in *LRP6* HBM compared to *LRP5* HBM.

3.4.2. DXA findings

DXA spine and hip BMD Z-scores were substantially elevated in all individuals with either of the two *LRP6* HBM mutations, ranging in Families 1 and 2 from +5.2 to +9.4 and +7.3 to +10.3 in the spine (mean +7.8) and +7.8 to +10.1 and +6.4 to +8.8 (mean +7.9) in the non-dominant hip, respectively (Ps < 0.0001) (Fig. 8).

Family 1: Radiographic Findings of *LRP6* HBM

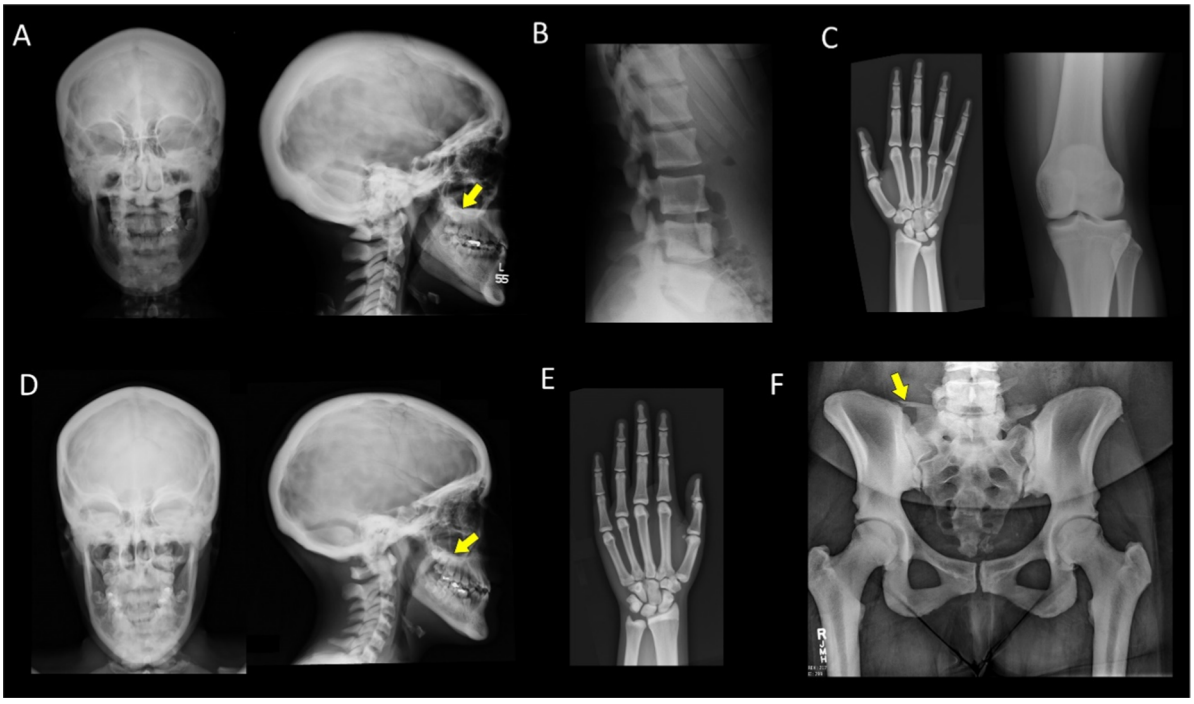

Proposita (III-1, Figure 1A):

A) At 19-years-old, the skull is extremely sclerotic and markedly thickened with prominent digital markings. It has uniformly dense diploic space without apparent trabecularizaton, a very dense base, sclerotic maxilla and roof of the mouth with torus palatinus apparent beneath the hard palate (arrow), anterior incisors and other teeth encased in bone, and mandible with an obtuse angle and protuberant mental tubercle. The maxilla is not hypoplastic and has teeth that project anteriorly with an "overbite". Cervical vertebral bodies and arches are osteosclerotic.

B) Lateral view of her lumbar spine shows diffuse osteosclerosis, including the neural arches, with some end-plate accentuation, but without the "rugger-jersey" spine of A-SD.

C) Her right distal radius shows some impaired tubulation (modeling), diffuse osteosclerosis, and cortical thickening, whereas her left knee is diffusely osteosclerotic with cortical thickening yet has normal external modeling.

Sister (III-3, Figure 1A):

D) At 15-years-old, the skull is sclerotic and thickened without visible diploic space or trabecularization. Its base is sclerotic, orbital roofs thickened, and petrous bones dense. The mandible has a thickened cortex. The lateral view shows a sclerotic maxilla with the anterior portion having prominent protruding teeth. The torus palatinus is readily apparent (arrow). Her incisors are encased in bone. The mandibular teeth especially are obscured by bone and the mental tubercle is prominent. The cervical spine is diffusely sclerotic.

E) Her left hand shows diffuse osteosclerosis, cortical thickening, and especially dense epiphyses.

Mother (II-2, Figure 1A):

F) At 43-years-old, the pelvis is diffusely osteosclerotic and has no "bone-in-bone" appearance. The femurs have a narrow medullary cavity and extremely wide cortices. The joint spaces are not narrowed. Multiple small exostoses are present, with one (arrow) extending from above the sacroiliac joint.

Fig. 6. Family 1: radiographic findings of *LRP6* HBM.

Regression analysis indicated that spine BMD Z-scores increased significantly with age for *LRP6* HBM ($P = 0.0448$, $R = +0.7183$) and perhaps A-SD ($P = 0.0563$, $R = +0.5025$), but not for *LRP5* HBM ($P = 0.9428$) (Table 3). For hip BMD Z-scores, no age effect was observed for any of the three groups (Ps > 0.05).

In the spine assessed by the GLM (Fig. 8), after adjustment for any age effect, the mean BMD Z-score was significantly higher in *LRP6* HBM (+7.8) compared to *LRP5* HBM (+6.5) ($P = 0.0403$). The *LRP6* HBM mean BMD Z-score in the spine ($P = 0.2779$) and hip ($P = 0.2612$) was not significantly different compared to A-SD. For A-SD, the only single

Family 2: Radiographic Findings of *LRP6* HBM

Propositus (III-1, Figure 1B):

A) At 8-years-old, the skull, facial bones, and hard palate are diffusely sclerotic. There is an "overbite".
B) The vertebral bodies and neural arches are diffusely sclerotic.
C) The pelvis and femurs are sclerotic and the femurs show cortical thickening and a narrowed medullary canal.
D) The external modeling of the sclerotic bones at the knees is normal.

Brother (III-2, Figure 1B):

E-G) At 6-years-old, the findings are the same as in the propositus, and the teeth are encased in dense bone and the anterior mandible is prominent.

Mother (II-2, Figure 1B):

H-K) At 36-years-old, the sons' principal findings are present, but her changes are more severe with the cortical widening and narrowing of the medullary cavities in the hands indicating disease progression with aging.
H) The craniofacial ratio appears normal. The torus palatinus (arrow) bulges into the mouth while not superiorly impacting the nasal cavity.
K) There is an exostosis (not osteochondroma) emanating from the distal left femur.

Grandmother (I-1, Figure 1B):

L-O) At 58-years-old, multiple small bony excrescences are present in the sclerotic pelvis (arrows).

Fig. 7. Family 2: radiographic findings of *LRP6* HBM.

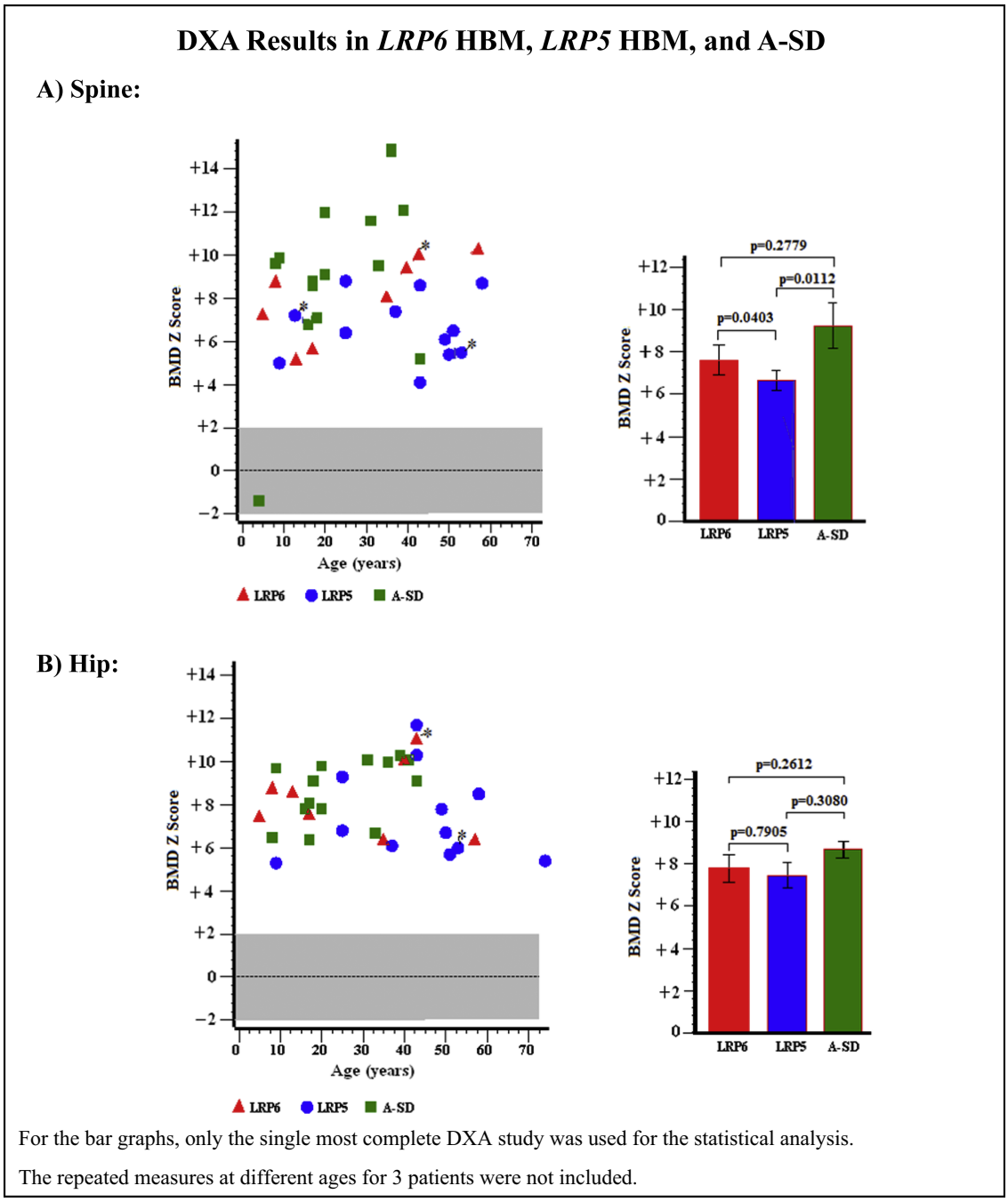

Fig. 8. DXA results in *LRP6* HBM, *LRP5* HBM, and A-SD.

Table 3
Spine and hip BMD Z-scores with aging for *LRP6* HBM, *LRP5* HBM, and A-SD.

Group	Mean age (years) (SD)	Range (min, max)	Age effect	
			Spine Z-score	Hip Z-score
LRP6	27.3 (19.0)	5.0, 57	Z = 6.1 + 0.072*age (R = +0.7183, P = 0.0448)	None (P = 0.9424)
LRP5	40.8 (18.5)	9.0, 74	None (P = 0.9428)	None (P = 0.8766)
A-SD	24.3 (12.7)	4.0, 43	Z = 4.2 + 0.24*age (R = +0.5025, P = 0.0563)	None (P = 0.0802)

BMD Z-score that was not elevated involved a normal value for the spine of a young child. The GLM showed no difference between *LRP6* HBM and *LRP5* HBM for hip mean BMD Z-scores (P = 0.7905) (Table 4). For A-SD, the mean BMD Z-score was greater compared to *LRP5* HBM for the spine (P = 0.0112), but not for the hip (P = 0.3080).

3.4.3. HR-pQCT findings

Cortical, trabecular, and total bone parameters were determined using the built-in Scanco software. HR-pQCT showed all individuals teenage or older with *LRP6* HBM had markedly elevated total and trabecular vBMD in both distal forearms and distal tibias that seemed to increase with subject age (Supplemental Table 1). The automated segmentation in the Scanco software was unable to fully distinguish cortical and trabecular compartments due to the remarkable increase in

Table 4
Spine and hip BMD Z-scores for *LRP6* HBM, *LRP5* HBM, and A-SD.

Group	SpineZ			HipZ			P values ($H_0 = 0$)
	Mean (SD)	95%CI	Min, Max	Mean (SD)	95%CI	Min, Max	
LRP6 (n = 7)	+7.8 (1.9)	6.1, 9.6	5.2, 10.3	+7.9 (1.3)	6.7, 9.2	6.4, 10.1	All Ps < 0.0001
LRP5 (n = 10)	+6.5 (1.5)	5.5, 7.6	4.1, 8.7	+7.7 (2.2)	6.0, 9.3	5.3, 11.7	
A-SD (n = 15)	+9.2 (4.0)	7.0, 11.5	−1.4, 14.9	+8.7 (1.4)	7.8, 9.5	6.4, 10.3	
P-values (comparisons with age effect adjusted)	P = 0.0403 (LRP6 vs LRP5)			P = 0.7905 (LRP6 vs LRP5)			
	P = 0.2779 (LRP6 vs A-SD)			P = 0.2612 (LRP6 vs A-SD)			
	P = 0.0112 (LRP5 vs A-SD)			P = 0.3080 (LRP5 vs A-SD)			

trabecular density. The values obtained for cortical vBMD thus appeared low-normal-to-normal when compared to published normal ranges by age because trabecular bone was being counted in the cortical segment (Fig. 9). This phenomenon was also observed in the artificially high cortical thickness values. BV/TV values for the distal radius and tibia were similarly elevated, ranging in the radius from 0.355 in the youngest subject to 0.555 in the oldest affected adult, and in the tibia from 0.398 to 0.514 in the youngest affected family members [32,33]. The μFEA showed highly elevated failure loads for all individuals with *LRP6* HBM at both sites, a phenomenon which also appears to increase and then plateau with age (Supplemental Table 2). Three-dimensional reconstructions showed loss of corticomedullary junction distinction from corticalization in all seven individuals with *LRP6* HBM (Fig. 9).

4. Discussion

We have discovered and delineated in two multigenerational families a new AD dento-osseous disorder [1], caused by heterozygous defects within *LRP6*, that can be distinguished with confidence from *LRP5* HBM only by mutation analysis. As discussed below, our findings support a role for *LRP6* in human skeletogenesis and provide some reassurance concerning anabolic treatments of skeletal disease aimed to enhance LRP5/LRP6-mediated signaling in osteoblasts.

4.1. LRP5 high bone mass

Several names denote *LRP5* HBM [1], which complicates literature searches for this rare but highly informative disorder. When identified in 1966 based on its clinical and radiographic features, *LRP5* HBM was first designated *hyperostosis corticalis generalisata congenita* by Worth and Wollin [34] to distinguish it from van Buchem disease [35] called *hyperostosis corticalis generalisata familiaris* [36]. Subsequently, *LRP5* HBM was sometimes referred to as "Worth-type" endosteal hyperostosis [37,38]. Then, by 2003, based on incorrect reports beginning in 1986 [18] that this endosteal hyperostosis was an OPT [3], "autosomal dominant osteopetrosis, type 1" became entrenched in the literature (OMIM #607634) [1]. Recently, *LRP5* HBM became classified also as van Buchem disease, type 2 [1] although never studied by van Buchem [35,36]. Thus, as reviewed below, we recommend this entity be called "*LRP5* HBM" because this term recognizes its etiology, principal feature, and distinguishes it from its "twin" *LRP6* HBM.

Discovery of the etiology of *LRP5* HBM leading to this renaming began in 1997 when Johnson et al. [21] studied a kindred from Nebraska, USA with a seemingly unique high bone mass trait they mapped to chromosome 11q12-13. At that time, we assessed their brief description of the clinical and radiographic findings as consistent with Worth-type endosteal hyperostosis [38]. Five years later in 2002, when Little et al. [10] discovered its genetic basis to be an *LRP5* missense mutation (p.G171V), the disorder became "HBM". Initially, its clinical findings were considered "non-syndromic" because affected individuals seemed healthy and without associated signs or symptoms [10]. However, later that year, Boyden et al. [11] reported from Connecticut, USA an unrelated second kindred that carried the identical *LRP5* mutation. They described the disorder as "syndromic" because affected individuals had a broad jaw and torus palatinus. *LRP5* HBM gained further notoriety because affected adults often said their dense bones prevented them from floating in water. Then, Whyte et al. [13] reported in 2004 an unrelated woman from Minnesota, USA harboring the identical *LRP5* mutation yet troubled by compression of several different cranial nerves, headache from Chiari I malformation, and exostoses surrounding her posterior teeth. Cranial nerve palsies are now well documented to sometimes complicate *LRP5* HBM [37]. In 2005, oropharyngeal exostoses were confirmed as another potential complication [15]. Now, 11 different *LRP5* mutations are reported [10–17] and variable expressivity is recognized for *LRP5* HBM.

4.2. LRP6 and human disease

Both *LRP5* (OMIM *603506) and *LRP6* (OMIM *603507) are expressed in many tissues [39]. Using the BLAST protein alignment tool, LRP5 and LRP6 are 70% identical and 83% homologous (excluding amino acids 1–18 of LRP6 and 1–30 of LRP5) (https://blast.ncbi.nlm.nih.gov).

Bi-allelic loss-of-function mutations of *LRP5* cause AR osteoporosis-pseudoglioma syndrome (OMIM #259770) [40]. Although bi-allelic *LRP6* loss-of-function mutations have not been reported in humans, *LPR6* null mice die at birth [41], suggesting this genetic situation might be identified only in abortuses or with perinatal lethality. However, some [42] heterozygous *LRP6* loss-of-function mutations have been identified (OMIM #610947) [1]. In 2007, such mono-allelic *LRP6* mutations were associated with AD coronary artery disease with atherosclerosis and features of the metabolic syndrome [43–45] such as hyperlipidemia, hypertension, and diabetes [43]. Beginning in 2015 [42], heterozygous loss-of-function mutations outside the region of *LRP6* that encodes the first β-propeller region of LRP6 (such as frameshift, splice site, and some missense mutations) were found to cause AD tooth agenesis and oligodontia [42,46,47]. In our *LRP6* HBM individuals, absence of adult maxillary lateral incisors suggests that either gain- or loss-of-function *LRP6* mutations can cause tooth agenesis. Other problems linked to heterozygous *LRP6* loss-of-function mutations include osteoporosis [48], spina bifida [49], and neural tube defects [50]. Furthermore, *LRP6* single nucleotide polymorphisms (SNPs) have been associated with BMD [51,52]. However, mutations have thus far been found throughout *LRP6* except where its first β-propeller is encoded.

4.3. Mouse models of LRP5 and LRP6 disease

As in humans, Lrp5 and Lrp6 in mice are cognate co-receptors with overlapping functions [7,23,41]. In mouse OBs, both proteins stimulate postnatal bone acquisition via Wnt signaling [5,6], and several murine models demonstrate the consequences from *Lrp5* and *Lrp6* inactivation [1]. *Lrp6* seems more important than *Lrp5* during mouse skeletal embryogenesis [7,23,41], because $Lrp6^{-/-}$ mice die at birth with truncation of the axial skeleton and limb defects whereas adult $Lrp5^{-/-}$ mice become osteoporotic [53]. Furthermore, OB-specific *Lrp6* knock-

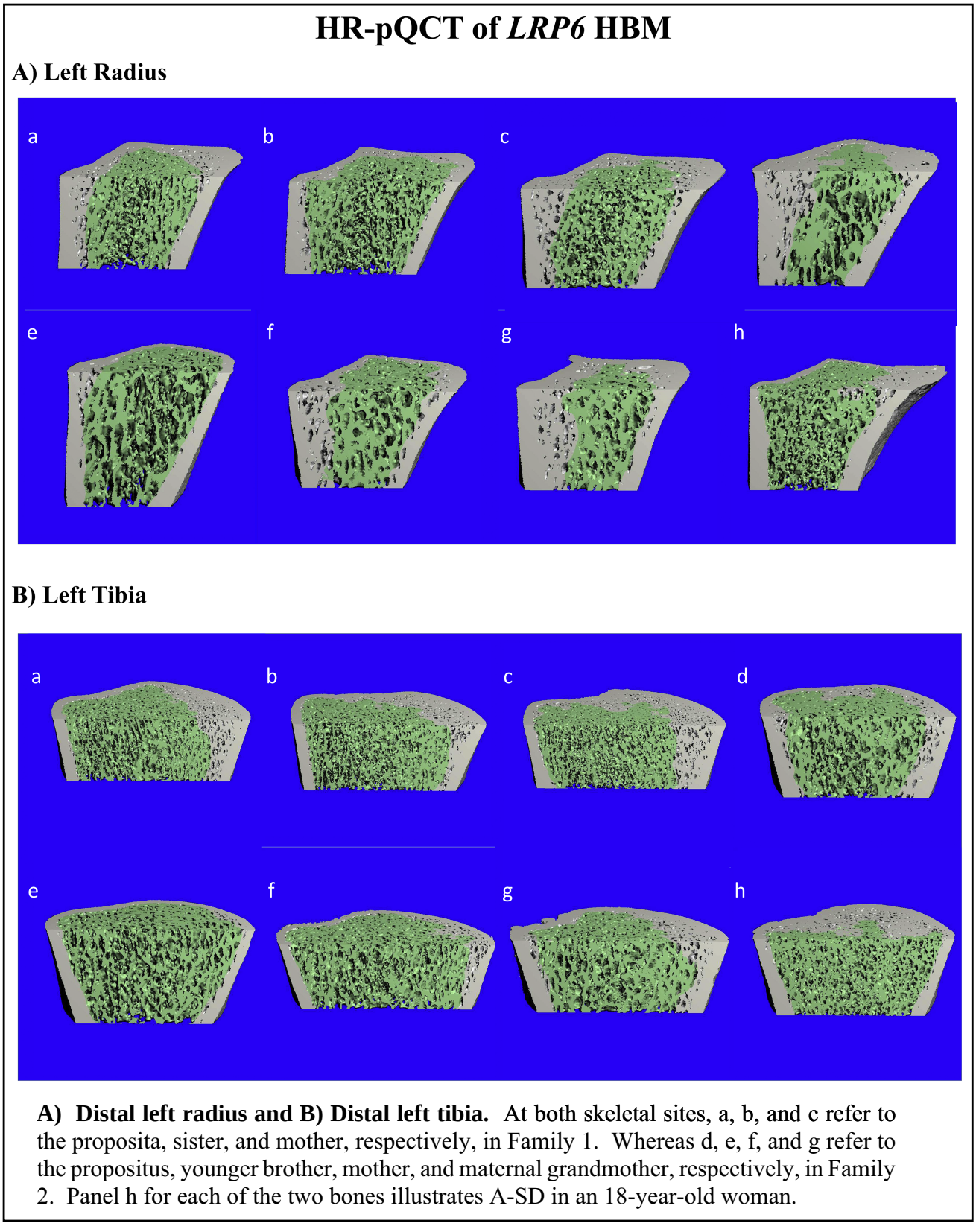

Fig. 9. HR-pQCT of *LRP6* HBM.

out mice failed to accumulate trabecular bone post-natally, whereas OB-specific *Lrp5* knock-out mice had normal trabecular bone volume at age eight weeks but lost bone tissue with aging [41]. Transgenic expression in mice of the murine homolog of the first identified *LRP5* missense mutation (G171V) resulted in HBM [54,55]. Notably, PTH bound to its receptor PTH1R in rats can complex with Lrp6 to increase bone formation [56]. Thus, Lrp6 can drive bone formation through either Wnt and perhaps PTH signaling.

4.4. LRP6 HBM vs LRP5 HBM

Family 1 and 2 each carry a heterozygous, but different, mutation in *LRP6*. Both missense defects match known *LRP5* HBM mutations (see below) [10–17]. We assessed whether *LRP6* HBM and *LRP5* HBM resemble each other, mindful there are differences between *Lrp6* versus *Lrp5* knock-out mice [7,23,41]. We found *LRP6* HBM and *LRP5* HBM to be indistinguishable in people based on the demographic, radiographic, and biochemical findings. Affected individuals in both HBM groups were all above average in height and had similar height Z-scores. However, investigation of more individuals with *LRP6* HBM and *LRP5* HBM will be necessary to know if tall stature is characteristic. Like *LRP5* HBM [11,13,15], *LRP6* HBM causes teeth to become encased in excessive bone, consistent with oropharyngeal exostoses, and we found exostoses were common elsewhere in the skeleton. When we spoke with two members of *LRP5* HBM Family 8 and one from Family 9, unlike for *LRP6* HBM they reported no absence of their adult maxillary lateral incisors. Perhaps this distinguishes between the disorders, but precise dental phenotyping of *LRP5* HBM and *LRP6* HBM requires future study. Although the spine mean BMD Z-score was statistically greater in *LRP6* HBM compared to *LRP5* HBM, the individual values overlapped. For hip BMD, there was no significant difference in the mean Z-scores. Although we found evidence for increasing BMD Z-scores with aging for *LRP6* HBM but not *LRP5* HBM or A-SD, all three disorders are rare and we could study only relatively few affected individuals. Further individuals with differing mutations must be investigated to know if *LRP6* HBM contrasts with *LRP5* HBM. Longitudinal investigation of our patients is planned to understand long-term outcomes. Importantly, *LRP6* HBM and *LRP5* HBM were both readily distinguished from the other principal type of AD elevated bone mass, A-SD [3], since only A-SD shows high circulating activity of a number of select enzymes. Furthermore, all seven study subjects with *LRP6* HBM considered themselves healthy although headaches and knee and bone pain sometimes troubled several of them, whereas *LRP5* HBM can be associated with cranial nerve palsies [13]. Other than the propositus in Family 2 who suffered a transient post-traumatic facial nerve palsy, these individuals with *LRP6* HBM offered no evidence of cranial nerve palsies. In contrast, our first *LRP5* HBM patient had been troubled by trigeminal neuralgia, facial nerve palsy, Chiari I malformation requiring craniectomy, oropharyngeal exostoses, and diffuse bone pain [13]. Blindness with raised intracranial pressure necessitating craniectomy in childhood was apparently a manifestation of *LRP5* HBM in an adult (Dr. Alan Burshell, personal communication).

Discovery of *LRP6* HBM enabled us to explore using "lipid panels" whether heterozygous gain-of-function of *LRP6* protects against the hyperlipidemia, atherosclerosis, and metabolic syndrome that can occur with heterozygous deactivation of *LRP6* [43–45]. Our data showed normal fasting glucose levels in all seven *LRP6* HBM individuals and one child and two adults with *LRP5* HBM. Furthermore, the lipid panels of Families 1 and 2 revealed no evidence of hypolipidemia, with instead hyperlipidemia documented in two individuals. Also, we did not find clinical or radiographic evidence of osteoarthritis or inflammatory joint destruction in our study subjects, although sclerostin deficiency can cause these problems in mice [57,58].

4.5. HR-pQCT

Challenges encountered scanning growing bones include determination and replication of the "region of interest" (ROI). For HR-pQCT, pediatric reference ranges for bone density based on sex, age, and ethnicity remain incomplete. In 2016, Burt et al. [33] published sex- and site-specific normative data for ages > 16 years. Gabel et al. in 2018 [32] published adolescent and young adult values using an ROI slightly different from ours. We followed the reference line placement and ROI selection of Burt and colleagues [33] using the standard adult protocol of Scanco Medical, Inc.

Although two of our *LRP6* HBM subjects were < age 16 years, major elevations [33] of bone density were obvious in all of them with this disorder. However, precise determination of cortical vBMD was obviated by apparent "corticalization" of the bone in the adjacent trabecular space. Nevertheless, for all of these individuals, total vBMD, trabecular vBMD, and failure load assessed by μFEA were markedly increased. Of interest, our 18-year-old patient with A-SD (#23A, Table 1) and similarly increased bone density measurements had a failure load disproportionately lower compared to bone density. While failure load determined from μFEA helps predict incident fractures [59], it is an imperfect assessment of bone quality and therefore strength. Still, our results from μFEA match better bone quality observed clinically in *LRP6* HBM compared to A-SD.

4.6. Conclusions

Elevated bone mass can be heritable [3]. In the study from 2016 by Gregson et al. [60] using next-generation sequencing for this phenotype, mutations found in known causal loci (including *LRP4*, *LRP5*, and *SOST*) explained only a small proportion of such individuals. Here, we discovered a new, yet anticipated, genetic disorder featuring dense bones but also unlikely to explain many such occurrences. Based on our longstanding experience with enigmatic cases of osteosclerosis and hyperostosis, only a relatively small number of such patients have *LRP6* HBM. Clearly, however, *LRP6* mutation analysis should now be added to gene panels aimed to identify dense bone disorders. Alternatively, *LRP6* could be examined by Sanger sequencing when *LRP5* analysis is negative, especially for a similar clinical phenotype. The generally healthy constitution of *LRP6* HBM helps narrow the differential diagnosis among the disorders featuring elevated bone mass [3,4]. Our findings seem informative for the development of anti-SOST and other treatments that would activate Wnt/β-catenin signaling in OBs to treat skeletal disorders. Headaches in *LRP6* HBM are concerning, but certainly less severe compared to the other disorders that result from *LRP5/LRP6* activation (sclerosteosis types 1 and 2 [61,62] and van Buchem disease [3]). *LRP6* HBM thus far seems associated with generally good health.

Author contributions

All authors helped write and approved the submitted manuscript. MPW was referred the patients for diagnosis, guided their evaluation, and drafted and finalized the manuscript. WHM delineated the radiological findings. FZ performed the statistical analyses. VNB analyzed the HR-pQCT data and helped reference and illustrate the manuscript. GSG, ELL, and AN coordinated the clinical investigations. MH and SD performed the mutation analyses directed and interpreted by SM. KD initially studied and then referred the proposita in Family 1.

Declaration of Competing Interest

The authors have nothing to disclose.

Acknowledgements

Our study was made possible by the skill and dedication of the nursing, laboratory, and radiology staff of the Center for Metabolic Bone Disease and Molecular Research, Shriners Hospital for Children, St. Louis, MO, USA. We thank physicians Jan Bruder, Alan Burshell, Jocelyn Hellig, Aliya Khan, Hussain Mahmud, Maithilee Menezes, and Michael Rickels for consulting us about their patients with *LRP5* HBM. Hiram Stahl performed the HR-pQCT scans, ran the analyses, and reviewed the HR-pQCT methodology. Ms. Sharon McKenzie provided expert secretarial help.

Appendix A. Supplementary data

Supplementary data to this article can be found online at https://doi.org/10.1016/j.bone.2019.05.003.

References

[1] Online Mendelian Inheritance in Man, OMIM®. McKusick-Nathans Institute of Genetic Medicine, Johns Hopkins University (Baltimore, MD), World Wide Web URL: http://omim.org/ , Accessed date: 2 January 2019.

[2] B. Frame, M. Honasoge, S.R. Kottamasu, Osteosclerosis, Dysostosis, and Related Disorders, Elsevier, New York, 1987.

[3] M.P. Whyte, Sclerosing bone disorders. Chapter 107, in: J.P. Bilezikian (Ed.), Primer on Metabolic Bone Diseases and Disorders of Mineral Metabolism, 9th ed., American Society for Bone and Mineral Research, Wiley-Blackwell, 2019, pp. 825–838.

[4] E. Boudin, W. Van Hul, Sclerosing bone disorders. Chapter 29, in: R.V. Thakker, M.P. Whyte, J. Eisman, T. Igarashi (Eds.), Genetics of Bone Biology and Skeletal Disease, 2nd ed., Elsevier (Academic Press), San Diego, CA, 2018, pp. 507–521.

[5] M.A. Rudnicki, B.O. Williams, Wnt signaling in bone and muscle, Bone 80 (2015) 60–66.

[6] T.A. Burgers, B.O. Williams, Regulation of Wnt/β-catenin signaling within and from osteocytes, Bone 54 (2013) 244–249.

[7] X. Li, Y. Zhang, H. Kang, W. Liu, P. Liu, J. Zhang, S.E. Harris, D. Wu, Sclerostin binds to LRP5/6 and antagonizes canonical Wnt signaling, J. Biol. Chem. 280 (2005) 19883–19887.

[8] B.M. Bhat, K.M. Allen, L. Wei, J. Graham, A. Morales, A. Anisowicz, H.-S. Lam, C. McCauley, V. Coleburn, M. Cain, E. Fortier, R.A. Bhat, F.J. Bex, P.J. Yaworsky, Structure-based mutation analysis shows the importance of LRP5 β-propeller 1 in modulating Dkk1-mediated inhibition of Wnt signaling, Gene 391 (2007) 103–112.

[9] M.-K. Chang, I. Kramer, T. Huber, B. Kinzel, S. Guth-Gundel, O. Leupin, M. Kneissel, Disruption of Lrp4 function by genetic deletion or pharmacological blockade increases bone mass and serum sclerostin levels, www.pnas.org/cgi/doi/10.1073/pnas.1413828111, (2014) (E5187-E5195).

[10] R.D. Little, J.P. Carulli, R.G. Del Mastro, J. Dupuis, M. Osborne, C. Folz, S.P. Manning, P.M. Swain, S.C. Zhao, B. Eustace, M.M. Lappe, L. Spitzer, S. Zweier, K. Braunschweiger, Y. Benchekroun, X. Hu, R. Adair, L. Chee, M.G. FitzGerald, C. Tulig, A. Caruso, N. Tzellas, A. Bawa, B. Franklin, S. McGuire, X. Nogues, G. Gong, K.M. Allen, A. Anisowicz, A.J. Morales, P.T. Lomedico, S.M. Recker, P. Van Eerdewegh, R.R. Recker, M.L. Johnson, A mutation in the LDL receptor-related protein 5 gene results in the autosomal dominant high-bone-mass trait, Am. J. Hum. Genet. 70 (2002) 11–19.

[11] L.M. Boyden, J. Mao, J. Belsky, L. Mitzner, A. Farhi, M.A. Mitnick, D. Wu, K. Insogna, R.P. Lifton, High bone density due to a mutation in LDL-receptor-related protein 5, N. Engl. J. Med. 346 (2002) 1513–1521.

[12] L. Van Wesenbeeck, E. Cleiren, J. Gram, R.K. Beals, O. Bénichou, D. Scopelliti, L. Key, T. Renton, C. Bartels, Y. Gong, M.L. Warman, M.C. De Vernejoul, J. Bollerslev, W. Van Hul, Six novel missense mutations in the LDL receptor-related protein 5 (LRP5) gene in different conditions with an increased bone density, Am. J. Hum. Genet. 72 (2003) 763–771.

[13] M.P. Whyte, W.R. Reinus, S. Mumm, High-bone-mass disease and LRP5 (letter), N. Engl. J. Med. 350 (2004) 2096–2098.

[14] L.M. Boyden, J. Mao, J. Belsky, L. Mitzner, A. Farhi, M.A. Mitnick, D. Wu, K. Insogna, R.P. Lifton, High bone density due to a mutation in LDL-receptor-related protein 5, N. Engl. J. Med. 346 (2004) 1513–1521.

[15] M.R. Rickels, X. Zhang, S. Mumm, M.P. Whyte, Oropharyngeal skeletal disease accompanying high bone mass and novel *LRP5* mutation, J. Bone Miner. Res. 20 (2005) 878–885.

[16] The Human Gene Mutation Database, http://www.hgmd.cf.ac.uk/ac/indix.php.

[17] K.M. Roetzer, G. Uyanik, A. Brehm, J. Zwerina, S. Azndieh, T. Czech, P. Roschger, B.M. Misof, K. Klaushofer, Novel familial mutation of LRP5 causing high bone mass: genetic analysis, clinical presentation, and characterization of bone matrix mineralization, Bone 107 (2018) 154–160.

[18] J. Bollerslev, T. Steiniche, F. Melsen, et al., Structural and histomorphometric studies of iliac crest trabecular and cortical bone in autosomal dominant osteopetrosis: a study of two radiological types, Bone 10 (1986) 19–24.

[19] E. Cleiren, B. Olivier, E. Van Hul, J. Gram, J. Bollerslev, F.R. Singer, K. Beaverson, A. Aledo, M. Whyte, T. Yoneyama, M.C. DeVernejoul, W. Van Hul, Albers-Schönberg disease (autosomal dominant osteopetrosis, type II) results from mutations in the *ClCN7* chloride channel gene, Hum. Mol. Genet. 10 (2001) 2861–2866.

[20] B.O. Williams, LRP5: from bedside to bench to bone, Bone 102 (2017) 26–30.

[21] M.L. Johnson, G. Gong, W. Kimberling, S.M. Recker, D.B. Kimmel, R.R. Recker, Linkage of a gene causing high bone mass to human chromosome 11 (11q12-13), Am. J. Hum. Genet. 60 (1997) 1326–1332.

[22] R.D. Little, R.R. Recker, M.L. Johnson, High bone density due to a mutation in LDL-receptor-related protein 5 (letter), N. Engl. J. Med. 347 (2002) 943.

[23] X. He, M. Semenov, K. Tamai, X. Zeng, LDL receptor-related proteins 5 and 6 in Wnt/β-catenin signaling: arrows point the way, Development 131 (2004) 1663–1677.

[24] V. Phatarakijnirund, S. Mumm, W.H. McAlister, D.V. Novack, D. Wenkert, K.L. Clements, M.P. Whyte, Congenital insensitivity to pain: fracturing without apparent skeletal pathobiology caused by an autosomal dominant, second mutation in scn11a encoding sodium channel 1.9, Bone 84 (2016) 289–298.

[25] M.P. Whyte, M. Griffith, L. Trani, S. Mumm, G.S. Gottesman, W.A.H. McAlister, K. Krysiak, R. Lesurf, Z.L. Skidmore, K.M. Campbell, I.S. Rosman, S. Bayliss, V.N. Bijanki, A. Nenninger, B.A. Van Tine, O.L. Griffith, E.R. Mardis, Melorheostosis: exome sequencing of an associated dermatosis implicates post-zygotic mosaicism of mutated KRAS, Bone 101 (2017) 145–155.

[26] S. Boutroy, M.L. Bouxsein, F. Munoz, P.D. Delmas, In vivo assessment of trabecular bone microarchitecture by high-resolution peripheral quantitative computed tomography, J. Clin. Endocrinol. Metab. 90 (2005) 6508–6515.

[27] J.B. Pialat, A.J. Burghardt, M. Sode, T.M. Link, S. Majumdar, Visual grading of motion induced image degradation in high resolution peripheral computed tomography: impact of image quality on measures of bone density and micro-architecture, Bone 50 (2012) 111–118.

[28] N. Vilayphiou, S. Boutroy, P. Szulc, B. van Rietbergen, F. Munoz, P.D. Delmas, R. Chapurlat, Finite element analysis performed on radius and tibia hr-pqct images and fragility fractures at all sites in men, J. Bone Miner. Res. 26 (2011) 965–973.

[29] M.P. Whyte, A. Chines, D.P. Silva, Y. Landt, J.H. Ladenson, Creatine kinase brain isoenzyme (BB-CK) presence in serum distinguishes osteopetroses among the sclerosing bone disorders, J. Bone Miner. Res. 11 (1996) 1438–1443.

[30] M.P. Whyte, L.G. Kempa, W.H. McAlister, F. Zhang, S. Mumm, D. Wenkert, Elevated serum lactate dehydrogenase isoenzymes and aspartate transaminase distinguish Albers-Schőnberg Disease (Chloride Channel 7 Deficiency Osteopetrosis) among the sclerosing bone disorders, J. Bone Miner. Res. 25 (2010) 2515–2526.

[31] S. Erkus, A. Turgut, O. Kose, Ö. Kalenderer, Management of early-onset hip osteoarthritis in an adolescent patient with osteopetrosis tarda: a case report, J. Pediatr. Orthop. B (2018), https://doi.org/10.1097/BPB.0000000000000583 Dec 21.

[32] L. Gabel, H.M. Macdonald, L.A. Nettlefold, H.A. McKay, Sex-, ethnic-, and age-specific centile curves for pQCT- and HR-pQCT-derived measures of bone structure and strength in adolescents and young adults, J. Bone Miner. Res. 33 (2018) 987–1000.

[33] L.A. Burt, Z. Liang, T.T. Sajobi, D.A. Hanley, S.K. Boyd, Sex- and site-specific normative data curves for HR-pQCT, J. Bone Miner. Res. 31 (2016) 2041–2047.

[34] H.M. Worth, D.G. Wollin, Hyperostosis corticalis generalisata congenita, J. Can. Assoc. Radiol. 17 (1966) 67–74.

[35] F.S.P. Van Buchem, H.N. Hadders, J.F. Hansen, M.G. Woldring, Hyperostosis corticalis generalisata: report of seven cases, Am. J. Med. 33 (1962) 387–397.

[36] F.S.P. Van Buchem, J.J.G. Prick, H.H.J. Jaspar, Hyperostosis Corticalis Generalisata Familiaris (Van Buchem's Disease). Excerpta Medica – Amsterdam-Oxford-New York, American Elsevier Publishing Co., New York, 1976.

[37] M.L. Kwee, W. Balemans, E. Cleiren, et al., An autosomal dominant high bone mass phenotype in association with craniosynostosis in an extended family is caused by LRP5 missense mutation, J. Bone Miner. Res. 20 (2005) 1254–1260.

[38] M.P. Whyte, Searching for gene defects that cause high bone mass, Am. J. Hum. Genet. 60 (1997) 1309–1311.

[39] E. Grünblatt, Z. Nemoda, A.M. Werling, A. Roth, N. Angyal, Z. Tarnok, H. Thomsen, T. Peters, An Hinney, J. Hebebrand, K.-P. Lesch, M. Romanos, S. Walitza, The involvement of the canonical Wnt-signaling receptor LRP5 and LRP6 gene variants with ADHD and sexual dimorphism: association study and meta-analysis, Am. J. Med. Genet. (2018) 1–12.

[40] Y. Gong, R.B. Slee, N. Fukai, G. Rawadi, S. Roman-Roman, A.M. Reginato, H. Wang, T. Cundy, F.H. Glorieux, D. Lev, M. Zacharin, K. Oexle, J. Marcelino, W. Suwairi, S. Heeger, G. Sabatakos, S. Apte, W.N. Adkins, J. Allgrove, M. Arslan-Kirchner, J.A. Batch, P. Beighton, G.C. Black, R.G. Boles, L.M. Boon, C. Borrone, H.G. Brunner, G.F. Carle, B. Dallapiccola, A. De Paepe, B. Floege, M.L. Halfhide, B. Hall, R.C. Hennekam, T. Hirose, A. Jans, H. Jüppner, C.A. Kim, K. Keppler-Noreuil, A. Kohlschuetter, D. LaCombe, M. Lambert, E. Lemyre, T. Letteboer, L. Peltonen, R.S. Ramesar, M. Romanengo, H. Somer, E. Steichen-Gersdorf, B. Steinmann, B. Sullivan, A. Superti-Furga, W. Swoboda, M.J. van den Boogaard, W. Van Hul, M. Vikkula, M. Votruba, B. Zabel, T. Garcia, R. Baron, B.R. Olsen, M.L. WarmanOsteoporosis-Pseudoglioma Syndrome Collaborative Group, LDL receptor-related protein 5 (LRP5) affects bone accrual and eye development, Cell 107 (2001) 513–523.

[41] R.C. Riddle, C.R. Diegel, J.M. Leslie, K.K. Van Koevering, M.-C. Faugere, T.L. Clemens, B.O. Williams, Lrp5 and Lrp6 exert overlapping functions in osteoblasts during postnatal bone acquisition, PLoS One 8 (2013) e63323.

[42] P.G. Maarten, M.P. Massink, M.A. Créton, F. Spanevello, W.M. Fennis, M.S. Cune, S.M. Savelberg, I.J. Nijman, M.M. Maurice, M.J. van den Boogaard, G. van Haaften, Loss-of-function mutation in the WNT coreceptor LRP6 cause autosomal dominant oligodontia, Am. J. Hum. Genet. 97 (2015) 621–626.

[43] A. Mani, J. Radhakrishnan, H. Wang, M.A. Mani, G. Nelson-Williams, K.S. Carew, S. Mane, H. Najmabadi, D. Wu, R.P. Lifton, LRP6 mutation in a family with early coronary disease and metabolic risk factors, Science 315 (2007) 1278–1282.

[44] R. Singh, E. Smith, M. Fathzadeh, W. Liu, G.W. Go, L. Subrahmanyan, S. Faramarzi, W. McKenna, A. Mani, Rare nonconservative LRP6 mutations are associated with metabolic syndrome, Hum. Mutat. 34 (9) (2013) 1221–1225.

[45] Y. Xu, W. Gong, J. Peng, H. Wang, J. Huang, H. Ding, D.W. Wang, Functional analysis LRP6 novel mutations in patients with coronary artery disease, PLoS One 9 (2014) e84345, , https://doi.org/10.1371/journal.pone.0084345.

[46] C.W. Ockeloen, K.D. Khandelwal, K. Dreesen, K.U. Ludwig, R. Sullivan, I.A.L.M. van Rooij, M. Thonissen, S. Swinnen, M. Phan, F. Conte, N. Ishorst, C. Gilissen, L. RoaFuentes, M. van de Vorst, A. Henkes, M. Steehouwer, E. van Beusekom, M. Bloemen, B. Vankeirsbilck, S. Bergé, G. Hens, J. Schoenaers, V.V. Poorten, J. Roosenboom, A. Verdonck, K. Devriendt, N. Roeleveldt, S.N. Jhangiani, L.E.L.M. Vissers, J.R. Lupski, J. de Ligt, J.W. Von den Hoff, R. Pfundt, H.G. Brunner, H. Zhou, J. Dixon, E. Mangold, H. van Bokhoven, M.J. Dixon, T. Kleefstra, A. Hoischen, C.E.L. Carels, Novel mutations in LRP6 highlight the role of WNT signaling in tooth agenesis, Genet. Med. 18 (2016) 1158–1162.

[47] N. Dinckan, R. Du, L.E. Petty, Z. Coban-Akdemir, S.N. Jhangiani, I. Paine, E.H. Baugh, A.P. Erdem, H. Kayserili, H. Doddapaneni, J. Hu, D.M. Muzny, E. Boerwinkle, R.A. Gibbs, J.R. Lupski, Z.O. Uyguner, J.E. Below, A. Letra, Whole-exome sequencing identifies novel variants for tooth agenesis, J. Dent. Res. 97 (2018) 49–59.
[48] B.O. Williams, K.L. Insogna, Where Wnts went: the exploding field of Lrp5 and Lrp6 signaling in bone, J. Bone Miner. Res. 24 (2009) 171–178.
[49] Y. Lei, K. Fathe, D. McCartney, H. Zhu, W. Yang, M.E. Ross, G.M. Shaw, R.H. Finnell, Rare LRP6 variants identified in spina bifida patients, Hum. Mutat. 36 (2015) 342–349.
[50] Z. Shi, X. Yang, B.B. Li, S. Chen, L. Yang, L. Cheng, T. Zhang, H. Wang, Y. Zheng, Novel mutation of LRP6 identified in Chinese Han population links canonical WNT signaling to neural tube defects, Birth Defects Res. 110 (2018) 63–71.
[51] A.-M. Sims, N. Shephard, K. Carter, T. Doan, A. Dowling, E.L. Duncan, J. Eisman, G. Jones, G. Nicholson, R. Prince, E. Seeman, G. Thomas, J.A. Wass, M.A. Brown, Genetic analyses in a sample of individuals with high or low BMD shows association with multiple Wnt pathway genes, J. Bone Miner. Res. 23 (2008) 499–506.
[52] J.B. Van Meurs, F. Rivadeneira, M. Jhamai, W. Hugens, A. Hofman, J.P. van Leeuwen, H.A. Pols, A.G. Uitterlinden, Common genetic variation of the low-density lipoprotein receptor-related protein 5 and 6 genes determines fracture risk in elderly white men, J. Bone Miner. Res. 21 (2006) 141–150.
[53] K.I. Pinson, J. Brennan, S. Monkley, B.J. Avery, W.C. Skarnes, An LDL receptor-related protein mediates Wnt signaling in mice, Nature 407 (2000) 535–538.
[54] P. Babij, Small C. Zhao w, Y. Kharode, P.J. Yaworsky, M.L. Bouxsein, P.S. Reddy, P.V. Bodine, J.A. Robinson, B. Bhat, J. Marzolf, F. Moran RA Bex, High bone mass in mice expressing a mutant LRP5 gene, J. Bone Miner. Res. 18 (2003) 960–974.
[55] Y. Zhang, Y. Wang, X. Li, J. Zhang, J. Mao, Z. Li, J. Zheng, L. Li, S. Harris, D. Wu, The LRP5 high-bone-mass G171V mutation disrupts LRP5 interaction with Mesd, Mol. Cell. Biol. 24 (2004) 4677–4684.
[56] M. Wan, C. Yang, J. Li, X. Wu, H. Yuan, H. Ma, X. He, S. Nie, C. Chang, X. Cao, Parathyroid horomone signaling through low-density lipoprotein-related proten 6, Genes Dev. 22 (2008) 2968–2979.
[57] W. Bouaziz, T. Funck-Brentano, H. Lin, C. Marty, H.-K. Ea, E. Hay, M. Cohen-Solal, Loss of sclerostin promotes osteoarthritis in mice via β-catenin-dependent and –independent Wnt pathways, Arthritis Res. Ther. 17 (2015) 24.
[58] C. Wehmeyer, S. Frank, D. Beckmann, M. Bottcher, C. Cromme, U. Konig, M. Fennen, A. Held, P. Paruzel, C. Hartmann, A. Stratis, A. Korb-Pap, T. Kamradt, I. Kramer, W. van den Berg, M. Kneissel, T. Pap, B. Dankbar, Sclerostin inhibition promotes TNF-dependent inflammatory joint destruction, www.ScienceTranslationMedicine.org 8 (2016) 330ra35.
[59] E.J. Samelson, K.E. Broe, H. Xu, L. Yang, S. Boyd, E. Biver, et al., Cortical and trabecular bone microarchitecture as an independent predictor of incident fracture risk in older women and men in the Bone Microarchitecture International Consortium (BoMIC): a prospective study, Lancet Diabetes Endocrinol. 7 (1) (2019) 34–43 Jan.
[60] C.L. Gregson, L. Wheeler, S.A. Hardcastle, L.H. Appleton, K.A. Addison, M. Brugmans, G.R. Clark, K.A. Ward, M. Paggoisi, M. Stone, J. Thomas, R. Agarwal, K.E. Poole, E. McCloskey, W.D. Fraser, E. Williams, A.N. Bullock, G. Davey Smith, M.A. Brown, J.H. Tobias, E.I. Duncan, Mutations in known monogenic high bone mass loci only explain a small proportion of high bone mass cases, J. Bone Miner. Res. 31 (2016) 640–649.
[61] M.P. Whyte, S.D. Amalnath, W.H. McAlister, R. Pedapati, V. Muthupillai, S. Duan, M. Husckey, V.N. Bijanki, S. Mumm, Sclerosteosis: report of type 1 or 2 in three Indian Tamil families and literature review, Bone 116 (2018) 321–332.
[62] O. Leupin, E. Piters, C. Halleux, S. Hu, I. Kramer, F. Morvan, T. Bouwmeester, M. Schirle, M. Bueno-Lozano, F.J. Fuentes, P.H. Itin, E. Boudin, F. de Freitas, K. Jennes, B. Brannetti, N. Charara, H. Ebersbach, S. Geisse, C.X. Lu, A. Bauer, W. Van Hul, M. Kneissel, Bone overgrowth-associated mutations in the LRP4 gene impair sclerostin facilitator function, J. Biol. Chem. 2011 (286) (2011) 19489–19500.